

The Mutation F227I Increases the Coupling of Metal Ion Transport in DCT1*

Received for publication, July 26, 2004, and in revised form, October 1, 2004
Published, JBC Papers in Press, October 7, 2004, DOI 10.1074/jbc.M408398200

Yaniv Nevo and Nathan Nelson‡

From the Department of Biochemistry, The George S. Wise Faculty of Life Sciences, Tel Aviv University,
Tel Aviv 69978, Israel

Metal ion transport by DCT1, a member of the natural resistance-associated macrophage protein family, is driven by protons. The stoichiometry of the proton to metal ion is variable, and under optimal transport conditions, more than 10 protons are co-transported with a single metal ion. To understand this phenomenon better, we used site-directed mutagenesis of DCT1 and analyzed the mutants by complementation of yeast suppressor of mitochondria import function-null mutants and electrophysiology with *Xenopus* oocytes. The mutation F227I resulted in an increase of up to 14-fold in the ratio between metal ions to protons transported. This observation suggests that low metal ion to proton transport of DCT1 resulting from a proton slippage is not a necessity of the transport mechanism in which positively charged protons are driving two positive charges of the metal ion in the same direction. It supports the idea that the proton slippage has a physiological advantage, and the proton slip was positively selected during the evolution of DCT1.

Metal ions are vital elements for all living cells. The NRAMP¹ family of metal ion transporters apparently plays a major role in metal ion homeostasis (1–4). Most of the information available about the mechanism of these transporters has resulted from studies of the family members NRAMP2 (DCT1) from mammalian and SMF1 from yeast expressed in *Xenopus* oocyte (5–9). *Xenopus* oocytes have a very low metal ion uptake background, which makes them the ideal heterologous expression system for metal ion transporters. In addition to the uptake measurements of the various divalent cations, it is possible to analyze the electrophysiological parameters generated by imposed potentials in the transporter-expressing oocyte as compared with control (10). The studies of DCT1 and Smf1p demonstrated that both of them function as general divalent metal ion transporters and that a proton gradient is the driving force for the metal ion transport (8, 9). However, the transport of protons and metal ions is “loosely coupled” because the process exhibits a variable stoichiometry. At pH 7 and membrane potentials of –90 to –30 mV, DCT1 transports one Fe²⁺ ion with one H⁺. At high proton concentration (low pH), the number of H⁺ ions transported with one Fe²⁺ ion increased to 10 (8). Moreover, on changing the membrane potential from

+10 to –80 mV at this low pH, the number of H⁺ ions transported with one Fe²⁺ ion increased from 3 to ~18 (9). In DCT1, this phenomenon was defined as a metal ion-dependent proton slippage (1, 9, 11). In contrast to DCT1, Smf1p showed a metal ion-independent sodium slip through the proton-translocating pathway (9, 12). The mechanism of this phenomenon is not well characterized, and the sites on the transporters that generate it are not known.

In this work, we addressed the coupling between proton and metal ion transport, and report on a mutation in DCT1 that exhibits an ~14-fold increase in the ratio of metal ion to proton transport.

MATERIALS AND METHODS

Site-directed Mutagenesis of DCT1—Oligonucleotide-directed, site-specific mutagenesis was performed by overlapping nucleotides with the mutation using the polymerase chain reaction (PCR) method (13). The DCT1 cDNA was cloned into pSPORT1 plasmid and was used as a template for PCR mutagenesis. NdeI and SpeI restriction sites were introduced at positions 145 and 1719 of the DCT1 reading frame (12). This resulted in the substitutions G50M, S573T, and V574S, which did not change the properties of DCT1. The mutation was confirmed by sequence analysis. The cRNAs of DCT1 and the mutants were synthesized by *in vitro* transcription from their cDNAs. Oocytes were injected with 50 μ l of water containing 50 ng of cRNA.

Oocyte Preparation and Uptake Measurements—*Xenopus laevis* oocytes were handled as described previously (12). Uptake experiments were performed 1–4 days following injections. The uptake solution for radiotracer experiments contained 100 mM NaCl, 10 mM Hepes, 2 mM Mes, 2 mM KCl, 1 mM CaCl₂, 1 mM MgCl₂, and 2 mM L-ascorbic acid, and the pH was adjusted to 5.5 with Tris base. Usually, 20 oocytes were incubated in 0.5 ml of a solution containing ⁵⁵FeCl₂, ⁵⁴MnCl₂, ⁶⁵ZnCl₂, or ⁶⁰CoCl₂. The radioactive tracer was usually mixed with 7–20 μ M unlabeled metal ion, and the uptake was followed for 30 min. The numbers given under “Results” are background-corrected and expressed in specific activity (pmol/oocyte/h).

Electrophysiological Experiments—Experiments utilizing the two-microelectrode voltage clamp technique were performed as described previously (14–16). Data analysis was performed as described previously (12). To analyze the pre-steady-state currents, the current traces were fitted to $I(t) = I_1 \exp(-t/\tau_1) + I_2 \exp(-t/\tau_2) + I_{ss}$, where I_1 is a capacitive current with time constant τ_1 associated with the oocyte plasma membrane (τ_1 is also observed in non-injected control oocytes), I_2 is a transient current associated with DCT1 expression with time constant τ_2 , and I_{ss} is the steady-state current. The parameters τ_1 , τ_2 , I_1 , I_2 , and I_{ss} were allowed to vary in all fits. The transient charge movements Q were obtained from the time integrals of $I_{\text{transient}}(t) = I_2 \exp(-t/\tau_2)$ during the on and off responses for all depolarizing and hyperpolarizing potentials and fitted by the Boltzmann equation, $Q = Q_{\text{max}}/[1 + \exp((V - V_{0.5})zF/RT)] + Q_{\text{hyp}}$, where Q_{max} represents the total charge movement, z represents the effective valence, $V_{0.5}$ represents the midpoint of the charge distribution, and Q_{hyp} represents the charge movement for extreme hyperpolarizing potentials (14, 15). R , T , and F are the usual thermodynamic constants.

Simultaneous Voltage-clamped Tracer and Current Measurements—Before the start of tracer uptake, the oocyte was clamped at –50 mV and perfused (washed) with substrate-free solution (that described above). After the perfusion was stopped, 50 μ l of the uptake solution

* The costs of publication of this article were defrayed in part by the payment of page charges. This article must therefore be hereby marked “advertisement” in accordance with 18 U.S.C. Section 1734 solely to indicate this fact.

‡ To whom correspondence should be addressed. Tel.: 972-3-640-6017; Fax: 972-3-640-6018, E-mail: nelson@post.tau.ac.il.

¹ The abbreviations used are: NRAMP, natural resistance-associated macrophage protein; Mes, 4-morpholineethanesulfonic acid; C, coulomb; TM, transmembrane.

containing $^{55}\text{Fe}^{2+}$ ($^{55}\text{FeCl}_2$ mixed with 20 μM unlabeled FeCl_2 to a final concentration of 26 μM) were added manually using a pipette, which washed out the substrate-free solution. The uptake lasted 3 min in the chamber, which volume was $\sim 50 \mu\text{l}$. To avoid dehydration, 1.5 min after the uptake began, another 50 μl of uptake solution was added. The uptake was terminated by perfusing the oocyte with the substrate-free solution. Currents were continuously measured during uptake. The oocyte was then dissolved in 50 μl of 10% SDS mixed with 4.5 ml of scintillation mixture, and the uptake activity was measured. The transported charge was calculated by integrating the Fe^{2+} -evoked current over the uptake period (3 min). Next, the charge:uptake and the metal ion to proton ratios were calculated. The transported charge (C, coulomb) was converted to the number of electric charges ($1 \text{ C} = 6.24 \times 10^{18} e^-$) and the uptake (pmol/oocyte/3 min) was converted to the number of Fe^{2+} ions that were transported (multiplying by Avogadro's number).

RESULTS

It has been shown that DCT1 and Smf1p function as general divalent metal ion transporters in mammals and yeast, respectively. Both use protons as their motive force to transport a broad-range of the same divalent metal ions and exhibit similar affinities for their various substrates (8, 12, 16). The mammalian DCT1 complements the phenotype of SMF1 null mutation in yeast (5, 17–19). The null mutant *smf1 Δ* is unable to grow in the presence of EGTA. Expression of Smf1p or the mammalian transporter DCT1 suppresses the above phenotype and allows growth of the yeast mutant in the presence of EGTA (18). Despite the relatively high homology, there are a few known differences between DCT1 and Smf1p. The most striking one is in the slips generated by the transporters, H^+ slip through DCT1 and Na^+ slip through Smf1p (11). The differences between the two homologues have to be due to the non-conserved amino acids in both proteins. Consequently, to locate the sites on the transporters responsible for this phenomenon, we substituted amino acids in DCT1 for the corresponding ones residing in Smf1p (19). It has been found that a mutation in the conserved glycine at position 216 (G216R) in the putative TM4 of DCT1 causes microcytic anemia in *mk-/-* mice and Belgrade rats (20). This mutation was subsequently shown to result in loss of Fe^{2+} transport ability (21). This suggests that the TM4 may have an important biological function. Therefore, we mutated the Phe-227 of DCT1, located in the same TM, to the corresponding isoleucine residue of Smf1p. The properties of the mutant were analyzed by expression in *Xenopus* oocytes, where measurements of uptake activity and electrophysiological parameters of the oocytes expressing the mutated transporter were recorded. In addition, the DCT1 mutant was tested for complementation of EGTA sensitivity of the Smf1p null mutants.

Metal Ion Uptake Activity of DCT1 and F227I Mutant—The uptake activity of Zn^{2+} , Fe^{2+} , Mn^{2+} , and Co^{2+} into the *Xenopus* oocytes expressing DCT1 and the F227I mutant is exhibited in Fig. 1. The data are representative of three experiments with oocytes from different frogs. The mutation did not result in any significant changes in uptake activity or specificity to the different metal ions, except for a small decrease in Co^{2+} uptake. Therefore, it was not surprising that the F227I mutant retained the capability to suppress the growth arrest of the yeast null mutant *smf1 Δ* in the presence of EGTA.² We generated more than thirty amino acid substitutions in DCT1, none of which exhibited the properties of F227I substitution described below.

Pre-steady-state Currents of DCT1 and the Mutation F227I—At pH 5.5 and a millisecond time scale, oocytes expressing DCT1 exhibited pre-steady-state currents, mainly at positively imposed potentials (8, 19). Pre-steady-state currents

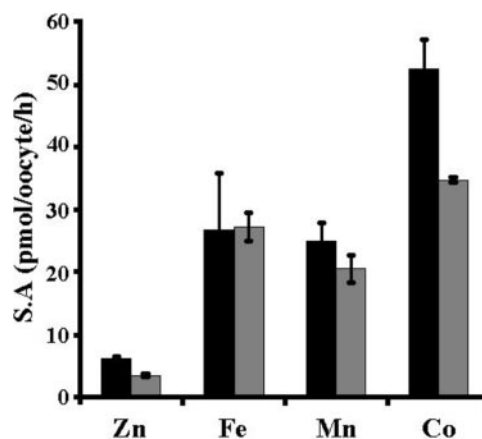


FIG. 1. Uptake of metal ions into *X. laevis* oocytes expressing the DCT1 and F227I mutant. The uptake experiment was performed at pH 5.5 in solution containing 100 mM NaCl, 2 mM KCl, 1 mM MgCl_2 , 1 mM CaCl_2 , 10 mM HEPES, 2 mM MES, 2 mM ascorbic acid, and the indicated metal ion in its chloride form at 7 μM , as described under "Materials and Methods." Black bars show the metal ion uptake into DCT1-expressing oocytes. Gray bars show the metal ion uptake into oocytes expressing the mutant F227I. The data for each bar represent means (after subtraction of the control values) + S.E. ($n = 20$). S.A., specific activity.

are an excellent indication of the expression level of transporters in *Xenopus* oocytes (10). The magnitude of the pre-steady-state currents recorded in oocytes injected with cRNA of native DCT1 or the mutant F227I (Fig. 2, A and C) indicated similar expression levels of the two transporters. To characterize the features of the F227I mutant, we subtracted the capacitative and steady-state currents to yield the transient current (Q) (Fig. 3B). At each applied voltage, time integration of the off transients yielded the charge moved. The charge-voltage (Q - V) relationship obtained (data not shown) was fitted to a single Boltzmann function (see "Materials and Methods"), and Q_{max} of 43 nC and $V_{0.5}$ of 42 mV were determined. Similar Q_{max} of 43 nC and a little higher $V_{0.5}$ of 49 mV were determined for native DCT1 (Fig. 3A). The time constant τ of the pre-steady-state current decay in F227I, in the potential jump from -25 to $+50$ mV, was 35 ms for the on response and 23 ms for the off response, and in DCT1, τ was 43 and 26 ms, respectively. According to the Q_{max} , $\sim 2.5 \times 10^{11}$ transporters were expressed on the plasma membrane of each oocyte expression DCT1 or F227I mutant. This calculation was made based on the mechanistic concept of transient charge movements in ion-coupled transporters that was proposed by Wright and co-workers (14, 22) for the Na^+ -coupled glucose transporter SGLT1 and the similarity between the pre-steady-state properties of SGLT1 and DCT1. Essentially, the pre-steady-state current results from imposed potential induction of occlusion and release of protons by DCT1 in the absence of substrate (1). The small decrease in $V_{0.5}$ and in τ_{on} of the mutation could indicate a small decrease in the affinity of the transporter to protons.

Metal Ion Induced Steady-state Currents in DCT1 and the Mutation F227I—The addition of Fe^{2+} , Mn^{2+} , and Co^{2+} to oocytes expressing DCT1 resulted in the disappearance of the pre-steady-state currents and appearance of large steady-state currents, especially at the negatively imposed potentials. At pH 5.5 and -80 mV, the coupling between H^+ and Fe^{2+} is interrupted, and the charge:uptake ratio is ~ 18 (9). The steady-state currents in those conditions are therefore mainly because of the protons transported (8, 9). The addition of Mn^{2+} to oocytes expressing the mutation F227I did abolish the pre-steady-state currents and generated only small steady-state currents compared with DCT1 (Fig. 2, B and D). At -125 mV,

² A. Cohen, unpublished results.

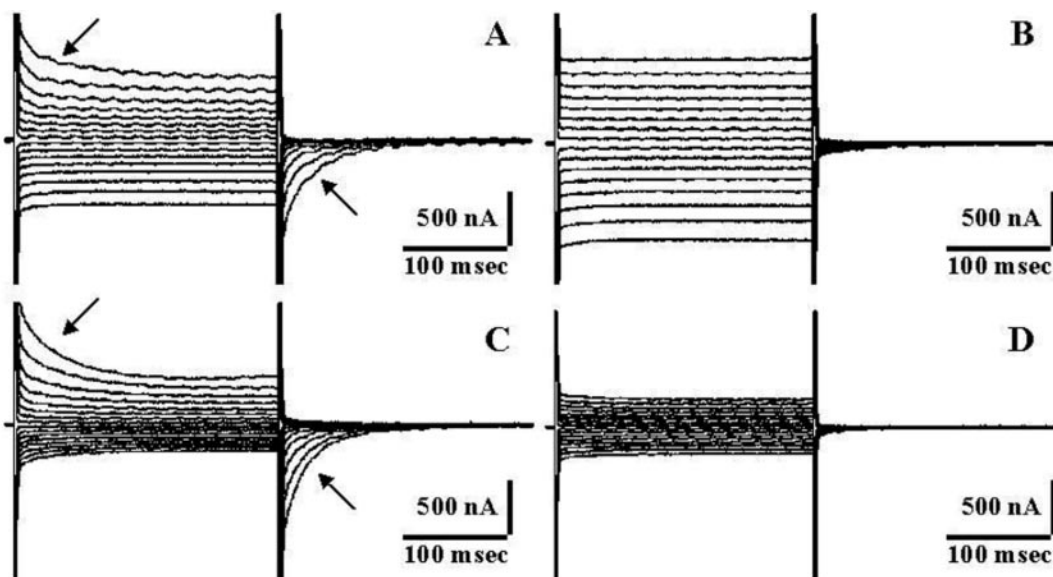


FIG. 2. The effect of Mn^{2+} on the pre-steady-state and steady-state currents in DCT1 and the F227I mutant. DCT1 and the mutant were expressed in *X. laevis* oocytes, and the currents were recorded in a solution similar to that described in the legend to Fig. 1, with or without 0.1 mM Mn^{2+} . The membrane voltage was transiently (500 ms) jumped to different imposed potentials, and the corresponding currents were recorded. The membrane potential was held at -25 mV and then jumped to varying potentials from $+50$ mV to -100 mV with 10-mV intervals. The transient currents are plotted against time, and the arrows indicate the pre-steady-state currents. A, DCT1. B, DCT1 + $MnCl_2$. C, F227I. D, F227I + $MnCl_2$. Control oocytes do not exhibit pre-steady-state currents.

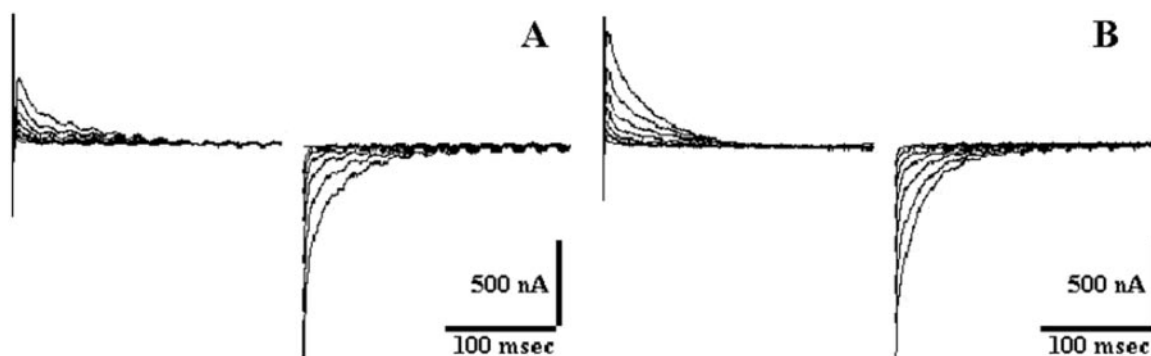


FIG. 3. Pre-steady-state charge movements were obtained from the total currents shown in Fig. 2 by subtraction of the capacitive and steady-state currents, using the fitted method (see "Materials and Methods"). A, DCT1. B, F227I mutant.

the addition of 0.1 mM Mn^{2+} induced an inward positive current of ~ 350 nA for DCT1 and a current of ~ 20 nA for the F227I mutant.

Simultaneous Measurement of Iron-induced Currents and Uptake Activity in DCT1 and the Mutation F227I—To further investigate these findings, we simultaneously measured the iron-induced currents and $^{55}Fe^{2+}$ uptake. First, the pre-steady-state currents were recorded in DCT1 and F227I expression oocytes that were bathed in substrate-free solution, pH 5.5 (Fig. 4A and C). The wild-type DCT1 and F227I mutant exhibited similar pre-steady-state currents. Addition of solution containing 20 μM of $FeCl_2$ resulted in the disappearance of the pre-steady-state currents and induced a steady-state current (Fig. 4, B and D). Fig. 5D shows the currents generated at different imposed potentials on DCT1 and its F227I mutant by the addition of $FeCl_2$. At -125 mV, the addition of Fe^{2+} induced a steady-state current of ~ 650 nA for DCT1 and only 75 nA for F227I mutant. Similar phenomenon was recorded between -25 and -125 mV. To analyze the amounts of charge movement in relation to metal ion uptake, we simultaneously traced the charge movement and $^{55}Fe^{2+}$ uptake in oocytes clamped at -50 mV. Fig. 5 shows the results of five different oocytes injected with DCT1 or F227I mutant. The charges that were transported during the 3-min exposure to 26 μM Fe^{2+}

were 25 μC and 2.3 μC , and the uptake activities were 7.25 pmol/oocyte/3 min and 5.4 pmol/oocyte/3 min for DCT1 and F227I, respectively. The charge:uptake ratio under these conditions (pH 5.5 and membrane potential of -50 mV) was calculated (see "Materials and Methods") to be 36 for DCT1 and 4.4 for the F227I mutant. Because each Fe^{2+} contributes two charges and each proton one charge, the number of protons transported with each metal ion is 34 for DCT1 and 2.4 for the F227I mutation. Hence, the mutation exhibits a 14-fold increase in the ratio of metal ion to proton transported. These observations suggest that the mutation F227I almost abolished the proton slip through DCT1 without statistically significant change in the metal ion transport activity.

Zinc Uptake Activity Exhibited by DCT1—At pH 5.5 and at -50 mV, divalent metals, including Zn^{2+} , generated similar inward currents of ≈ 100 nA in oocytes expressing DCT1 (1, 12). Moreover, Zn^{2+} inhibits Fe^{2+} and Mn^{2+} uptakes in oocytes expressing DCT1 or Smf1p and in yeast cells expression Smf1p (5, 8, 12). However, in previous studies, we could not detect $^{65}Zn^{2+}$ uptake into *Xenopus* oocytes expressing DCT1 or Smf1p (12, 19). These observations were in line with results from other studies with DCT1 expressed in Caco-2 TC7 cells, which suggest that Zn^{2+} is not transported by DCT1 (23). We therefore concluded that Zn^{2+} binds to the transporter, probably to

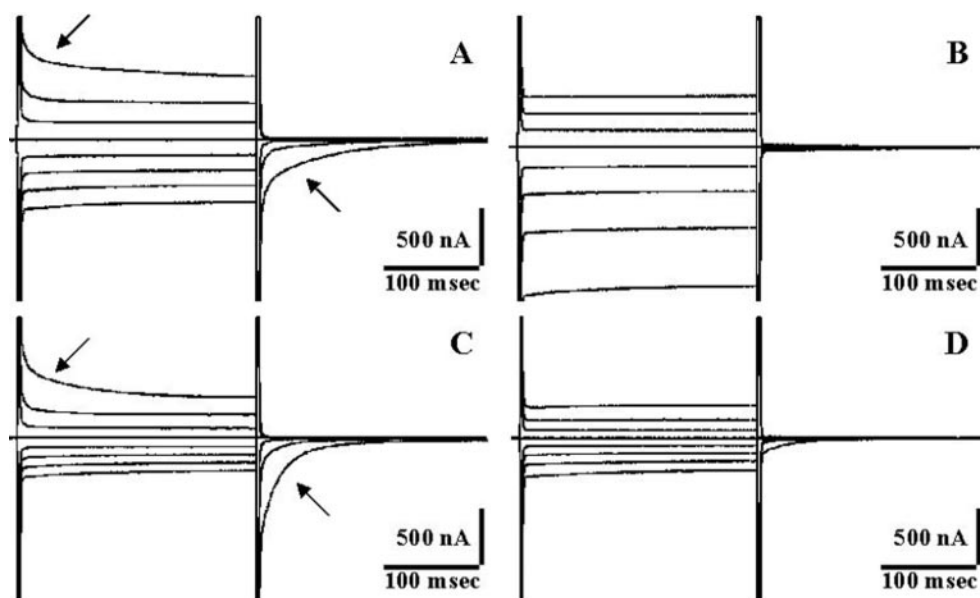
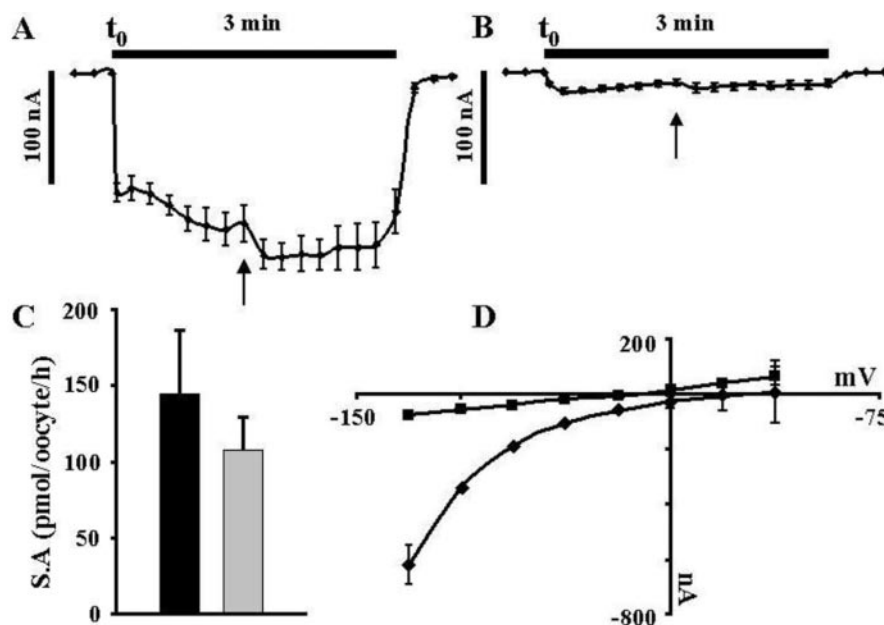


FIG. 4. The effect of Fe^{2+} on the pre-steady-state and steady-state currents in DCT1 and the F227I mutant. DCT1 and the mutant were expressed in *X. laevis* oocytes. The experimental conditions were as described in the legend to Fig. 2, except that, instead of Mn^{2+} , Fe^{2+} at $20 \mu\text{M}$ was added as specified, and the membrane voltage was held at -25 mV and then jumped to varying potentials from $+50 \text{ mV}$ to -125 mV with 25 mV intervals. The transient currents are plotted against time, and the arrows indicate the pre-steady-state currents. A, DCT1. B, DCT1 + FeCl_2 . C, F227I. D, F227I + FeCl_2 . Control oocytes do not exhibit pre-steady-state currents.

FIG. 5. Simultaneous measurement of iron-induced currents and uptake activity into *X. laevis* oocytes expressing DCT1 and the F227I mutant. The experiment was performed as described under "Materials and Methods." The second addition of $50 \mu\text{l}$ of uptake solution is marked with an arrow. A, the iron-induced currents recorded for oocytes expressing DCT1. B, the iron-induced currents recorded for the F227I mutant. C, the iron uptake activity measured for the oocyte expressing DCT1 (black bar) and the F227I mutant (gray bar). D, the differential currents in the presence and absence of the Fe^{2+} measured in Fig. 4 were plotted against membrane voltage. Diamonds, DCT1; squares, F227I mutant. The data for each point and bar represent means (after subtraction of the control values) + S.E. (for A, B, and C, $n = 5$; and for D, $n = 3$). S.A., specific activity.



the same site as the other metal ions, and generates the proton slip through DCT1 but does not transport. In this work, we contradicted our previous findings, since we recently detected $^{65}\text{Zn}^{2+}$ uptake into oocytes expressing DCT1, in agreement with the recently published data by Marciani *et al.* (24). As depicted in Figs. 1 and 6A, the values of $^{65}\text{Zn}^{2+}$ uptake activity were $\sim 10 \text{ pmol/oocyte/h}$. We measured the uptake activity of Fe^{2+} and Zn^{2+} during various days after the injection of DCT1 cRNA to the oocytes (Fig. 6A). As shown in Fig. 6C, the ratio between Zn^{2+} and Fe^{2+} uptake was altered during the various days, from $\sim 3\%$ on the first day to $\sim 30\%$ on the fourth day. The ratio between Mn^{2+} and Fe^{2+} was also altered, from 30% on the first day to 116% on the fourth day (data not shown). Although Fe^{2+} uptake activity reached steady-state 2 days after injection, Zn^{2+} and Mn^{2+} uptake activities continued to rise even 4 days after injection. The data are representative of four experiments with oocytes from different frogs. Reduction

of the amount of cRNA that was injected into the oocytes, to an amount that is under the saturation level, did indeed reduce the uptake activity but did not change these ratios (data not shown). This phenomenon did not occur when we measured the uptakes of two substrates, GABA and betaine, by the GABA transporter GAT3.³ These results can be explained either by oligomerization or by conformation changes in DCT1 that occur during the time of its presence in the plasma membrane, which altered the specificity of the transporter to the various substrates.

DISCUSSION

The family of NRAMP metal ion transporters plays a major role in metal ion homeostasis (2–4, 25). We developed a concerted approach to the study of Smf1p and DCT1. It employs

³ E. Kfir, unpublished results.

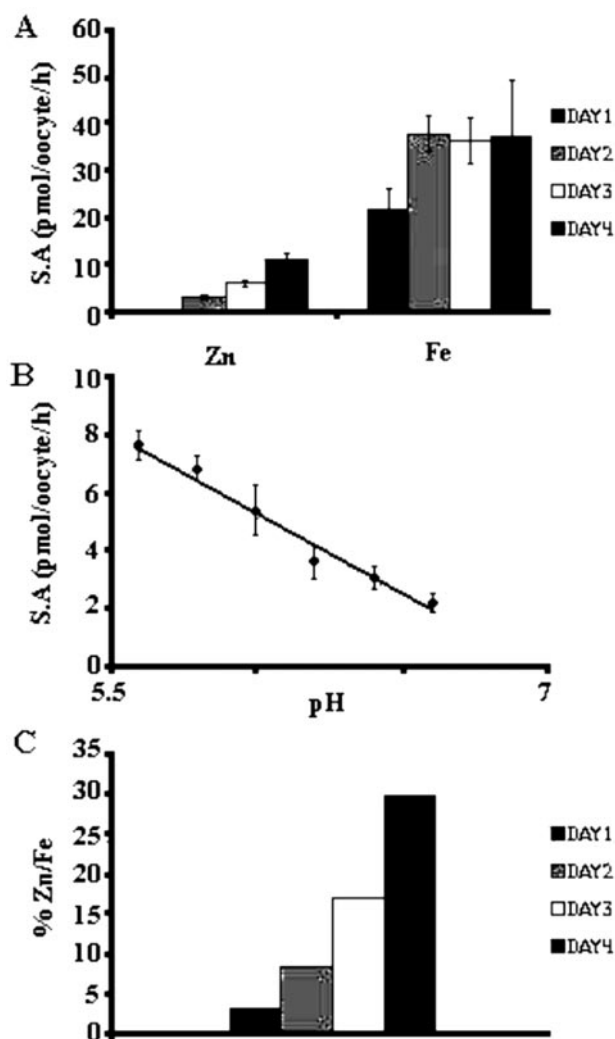


FIG. 6. Characterization of zinc uptake activity into *X. laevis* oocytes injected with mRNA of DCT1. The experimental conditions were as described in the legend to Fig. 1. A, uptake of zinc and iron 1–4 days after the injection. B, zinc uptake activity by DCT1 at different pH values ($R^2 = 0.98$). The data for each bar and pH point represent means (after subtraction of the control values) + S.D. ($n = 20$). C, the ratio (in percent) between Zn^{2+} and Fe^{2+} uptake activity 1–4 days after injection. S.A., specific activity.

yeast null mutants lacking the SMF metal ion transporters (18) and *Xenopus* oocytes as an expression system for Smf1p and DCT1 (12). Using this approach, we investigated the first external loop of DCT1. The properties of various mutants in this region suggest that loop 1 is involved in the metal ion binding and its coupling to the proton-driving force (19). One of the prominent mechanistic properties of these transporters is the proton slip through DCT1 and the Na^+ slip through Smf1p (11). Under conditions of neutral pH and/or neutral membrane potential, DCT1 would be in the coupled state; that is, the stoichiometry of proton:metal ion transport would be close to 1:1. Increasing the driving force, by either reducing the pH or increasing the negative potential, generates a proton slip, which maintains the levels of substrate transport at rates that are close to the “normal” rates of the coupled state. However, it simultaneously increases the rate of proton movement through the transporter. A similar mechanism applies to Smf1p-mediated slippage, except that here the ion that slips is Na^+ . Metal ion transport by Smf1p is also driven by proton motive force, and inhibition of the latter by Na^+ results in reduced metal ion uptake. The physiological significance of this phenomenon in metal ion transporters could be protection of cells against the

excessive transporting of these elements. Such a mechanism is necessary when cells are exposed to conditions of abundant metals and acidic environment. The mechanism of this phenomenon is not well characterized, and the sites on the transporters generating this phenomenon are not known. To locate these sites, we attempted to gain control over the slippage magnitude by reciprocal amino acid substitution between DCT1 and Smf1p. We managed to diminish the proton slip through DCT1 by substituting a single amino acid (F227I). This mutation did not generate any Na^+ slip, and the transporter properties were not influenced by the removal of Na^+ from the medium (not shown).

The amino acid Phe-227 is located in the putative TM4 of DCT1 that may be situated in close proximity to the proton pathway of the transporter. This notion is in line with a previous study that demonstrated the importance of TM4 for the function of the transporter (20, 21). The mutation F227I did not result in any significant changes in the uptake activity or specificity of the different metal ions, except for a small decrease in Co^{2+} uptake. It was therefore not surprising that the F227I mutant retained the capability to suppress the growth arrest of *smf1Δ* in a medium containing EGTA. When expressed in *Xenopus* oocytes, the Q_{max} value of the F227I mutant was comparable with that of native DCT1, indicating that the expression levels of the mutant are similar to those of the native DCT1.

The coupling between the driving force and substrate transport may be modulated by different physiological conditions (11). However, for most of the transporters studied so far, a fixed number of driving ions are reported to cross the membrane per the single substrate molecule that is transported (26–29). Even for proliferated families of transporters, such as the Na^+/Cl^- neurotransmitter transporters, stoichiometric amounts of Na^+ , Cl^- , and substrate are reported (30–33). Different transporters in this family operate with unique stoichiometries, and some of them even utilize K^+ as part of the driving force (34–36). In contrast, transporters such as the *Escherichia coli* lactose permease were reported to operate with a fixed stoichiometry of 1 for the symport of proton and lactose (37). Studies involving site-directed mutagenesis yielded numerous mutants in which the properties of proton and/or the substrate transport were modified (19, 38, 39). One of these mutants, E269D, is of particular interest to this discussion (40–42). This delicate mutation, which changed the position of a carboxylic acid by 1.5 Å, led to a few changes in the transport properties of lactose permease. The changes included reduction of the coupling between proton to lactose transport, such that ~10 protons had to cross the transporter for each lactose. This proton slippage is comparable with the native slip of DCT1.

The mild mutation F227I in DCT1 resulted in marked reduction in the proton slip through DCT1 and essentially mimicked the reversal of the E269D mutation in lactose permease (40–42). The effect of the F227I mutation may also be analogous to the one of E269D, except that in the former it may induce a conformational change that cancels the slip that was evolutionarily selected for the benefit of the physiology of metal ion transport in the mammalian duodenum (11). Further studies will be required to identify the proton translocation pathway that was influenced by the F227I mutation in DCT1.

REFERENCES

- Nelson, N. (1999) *EMBO J.* **18**, 4361–4371
- Forbes, J. R., and Gros, P. (2001) *Trends Microbiol.* **9**, 397–403
- Van Ho, A., Ward, D. M., and Kaplan, J. (2002) *Annu. Rev. Microbiol.* **56**, 237–261
- Goswami, T., Rolf, A., and Hediger, M. A. (2002) *Biochem. Cell Biol.* **80**, 679–689
- Supek, F., Supekova, L., Nelson, H., and Nelson, N. (1996) *Proc. Natl. Acad. Sci. USA* **93**, 1111–1116

- Sci. U. S. A.* **93**, 5105–5110
6. Supek, F., Supekova, L., Nelson, H., and Nelson, N. (1997) *J. Exp. Biol.* **200**, 321–330
 7. Liu, X. F., Supek, F., Nelson, N., and Culotta, V. C. (1997) *J. Biol. Chem.* **272**, 11763–11769
 8. Gunshin, H., Mackenzie, B., Berger, U. V., Gunshin, Y., Romero, M. F., Boron, W. F., Nussberger, S., Gollan, J. L., and Hediger, M. A. (1997) *Nature* **388**, 482–488
 9. Chen, X.-Z., Peng, J.-B., Cohen, A., Nelson, H., Nelson, N., and Hediger, M. A. (1999) *J. Biol. Chem.* **274**, 35089–35094
 10. Wright, E. M., Loo, D. D., Panayotova-Heiermann, M., Lostao, M. P., Hirayama, B. H., Mackenzie, B., Boorer, K., and Zampighi, G. (1994) *J. Exp. Biol.* **196**, 197–212
 11. Nelson, N., Sacher, A., and Nelson, H. (2002) *Nat. Rev. Mol. Cell Biol.* **3**, 876–881
 12. Sacher, A., Cohen, A., and Nelson, N. (2001) *J. Exp. Biol.* **204**, 1053–1061
 13. Noumi, T., Beltrán, C., Nelson, H., and Nelson, N. (1991) *Proc. Natl. Acad. Sci. U. S. A.* **88**, 1938–1942
 14. Loo, D. D., Hazama, A., Supplisson, S., Turk, E., and Wright, E. M. (1993) *Proc. Natl. Acad. Sci. U. S. A.* **90**, 5767–5771
 15. Loo, D. D., Hirayama, B. A., Gallardo, E. M., Lam, J. T., Turk, E., and Wright, E. M. (1998) *Proc. Natl. Acad. Sci. U. S. A.* **95**, 7789–7794
 16. Chen, X.-Z., Shayakul, C., Berger, U. V., Tian, W., and Hediger, M. A. (1998) *J. Biol. Chem.* **273**, 20972–20981
 17. Pinner, E., Gruenheid, S., Raymond, M., and Gros, P. (1997) *J. Biol. Chem.* **272**, 28933–28938
 18. Cohen, A., Nelson, H., and Nelson, N. (2000) *J. Biol. Chem.* **275**, 33388–33394
 19. Cohen, A., Nevo, Y., and Nelson, N. (2003) *Proc. Natl. Acad. Sci. U. S. A.* **100**, 10694–10699
 20. Fleming, M. D., Trenor, C. C., III, Su, M. A., Foernzler, D., Beier, D. R., Dietrich, W. F., and Andrew, N. C. (1997) *Nat. Genet.* **16**, 383–386
 21. Fleming, M. D., Romano, M. A., Su, M. A., Garrick, L. M., Garrick, M. D., and Andrews, N. C. (1998) *Proc. Natl. Acad. Sci. U. S. A.* **95**, 1148–1153
 22. Mackenzie, B., Loo, D. D., Fei, Y., Liu, W., Ganapathy, V., Leibach, F. H., and Wright, E. M. (1996) *J. Biol. Chem.* **271**, 5430–5437
 23. Tandy, S., Williams, M., Leggett, A., Lopez-Jimenez, M., Dedes, M., Ramesh, B., Srai, S. K., and Sharp, P. (2000) *J. Biol. Chem.* **275**, 1023–1029
 24. Marciani, P., Trotti, D., Hediger, M. A., and Monticelli, G. (2004) *J. Membr. Biol.* **197**, 92–99
 25. Cellier, M., Prive, G., Belouchi, A., Kwan, T., Rodrigues, V., Chia, W., and Gros, P. (1995) *Proc. Natl. Acad. Sci. U. S. A.* **92**, 10089–10093
 26. McGivan, J. D., and Pastor-Anglada, M. (1994) *Biochem. J.* **299**, 321–334
 27. Inoue, K., Fei, Y. J., Zhuang, L., Gopal, E., Miyauchi, S., and Ganapathy, V. (2004) *Biochem. J.* **378**, 949–957
 28. Bers, D. M., and Weber, C. R. (2002) *Ann. N. Y. Acad. Sci.* **976**, 500–512
 29. Blair, D. F. (2003) *FEBS Lett.* **545**, 86–95
 30. Nelson, N. (1998) *J. Neurochem.* **71**, 1785–1803
 31. Keynan, S., Suh, Y.-J., Kanner, B. I., and Rudnick, G. (1992) *Biochemistry* **31**, 1974–1979
 32. Lester, H. A., Cao, Y., and Mager, S. (1996) *Neuron* **17**, 807–810
 33. Clark, J. A., Deutch, A. Y., Gallipoli, P. Z., and Amara, S. G. (1992) *Neuron* **9**, 337–348
 34. Rudnick, G., and Nelson P. J. (1978) *Biochemistry* **17**, 4739–4742
 35. Rudnick, G. (1997) in *Neurotransmitter Transporters-Structure, Function, and Regulation* (Reith, E. A., ed) pp. 73–100, Humana Press, Totowa, New Jersey
 36. Gu, H. H., Wall, S., and Rudnick, G. (1996) *J. Biol. Chem.* **271**, 6911–6916
 37. Sahin-Tóth, M., Karlin, A., and Kaback, H. R. (2000) *Proc. Natl. Acad. Sci. U. S. A.* **97**, 10729–10732
 38. Kaback, H. R., Sahin-Toth, M., and Weinglass, A. B. (2001) *Nat. Rev. Mol. Cell Biol.* **2**, 610–620
 39. Lam-Yuk-Tseung, S., Govoni, G., Forbes, J., and Gros, P. (2003) *Blood* **101**, 3699–3707
 40. Weinglass, A. B., Whitelegge, J. P., Hu, Y., Verner, G. E., Faull, K. F., and Kaback, H. R. (2003) *EMBO J.* **22**, 1467–1477
 41. Franco, P. J., and Brooker, R. J. (1994) *J. Biol. Chem.* **269**, 7379–7386
 42. Ujwal, M. L., Sahin-Tóth, M., Persson, B., and Kaback, H. R. (1994) *Mol. Membr. Biol.* **11**, 9–16